

A Multifractal Detrended Fluctuation Analysis-Based Framework for Fault Diagnosis in Autonomous Microgrids

S. Pratiher, M. Mukherjee and N. Haque

Abstract The time series obtained during different fault events in an inverter-based microgrid are known to be inherently nonlinear, non-stationary and exhibits multifractal, chaotic behavior. This paper proposes a novel feature extraction and fault detection methodology based on multifractal detrended fluctuation analysis (MFDFA). The limitations of single-scale detrended fluctuation analysis and its susceptibility to interfere with the background noises are overcome in MFDFA which characterizes the multi-scaling nonlinear behavior of load signals during faults. The shape and distribution of the multifractal spectrum along with Hurst exponent are extracted from MFDFA analysis for pattern recognition and classification of different fault events. The efficacy of multifractal features in fault detection and localization with artificial neural network (ANN)-based classifier validates the adequacy of the proposed model.

Keywords Detrended fluctuation analysis · Multifractal spectrum
Microgrids · Power system faults · ANN

S. Pratiher (✉)

Department of Electrical Engineering, Indian Institute of Technology,
Kanpur, Uttar Pradesh, India
e-mail: sawon1234@gmail.com

S. Pratiher

Department of Mathematics, Indian Institute of Technology, Kharagpur,
West Bengal, India

M. Mukherjee · N. Haque

Department of Electrical Engineering, Jadavpur University, Kolkata,
West Bengal, India

M. Mukherjee

School of Electrical Engineering & Computer Science,
Washington State University, Pullman, USA

© Springer Nature Singapore Pte Ltd. 2018

R. Bera et al. (eds.), *Advances in Communication, Devices and Networking*,
Lecture Notes in Electrical Engineering 462,
https://doi.org/10.1007/978-981-10-7901-6_24

1 Introduction

The rapid progress in the distributed power generation sector has led to the establishment of microgrids, which in turn has accelerated the feasibility of power supply to locally spaced loads by distributed means. These microgrids are formed by clustering a number of power electronic devices that converts the dc power generated by photo voltaic cells, fuel cells, etc., to ac power for local utilization, thereby unleashing autonomous power systems. Overall, these microgrids provide substantial reliability and efficiency to the underlying power system but these are prone to power system transients like faults and voltage dips due to their inherent negligible physical inertia. So, a proper fault detection and protection mechanism is a crucial aspect for autonomous microgrid operation [1, 2].

Now, a microgrid can operate in a grid connected mode or an islanded mode. For a grid connected mode, voltage and frequency of the microgrid are primarily determined by the main grid [3]. Whereas, in case of a microgrid operating in an islanded mode, majority of the faults arises from within the microgrid arises, and hence, fault detection becomes difficult. In a larger network of interconnections, the magnitude of fault current is very high and so, faults are easily detectable [4]. Whereas in an inverter-based microgrid operating in an islanded mode fault detection is difficult as the inverters are only able to supply fault currents that are only twice of the rated value [5]. Thus, traditional over current relay-based protection systems are inadequate for fault detection. To overcome this difficulty, different solutions were proposed. This can be solved by enhancing the fault current by increasing the inverter capacity or by incorporating energy storage elements [6]. Also suitable feature vectors can be determined and trained with machine learning tools for identifying fault conditions. Statistical machine learning tools like support vector machines (SVMs) and principal component analysis (PCA) have shown competence as fault localization [7, 8]. In this paper, we have utilized an artificial neural network-based learning model using multifractal features of fault events for fault segregation.

The paper is organized in the following sections. Section 2 provides a dynamic model for an inverter-based microgrid. An autonomous microgrid model comprising of three inverters and domestic loads interconnected by a network has been developed. In Sect. 3, the underlying theory for the non-stationary fault events, their fractal parameter extraction and classification using neural network is discussed. Results obtained from different kinds of simulated faults are discussed in Sect. 4. Finally, the possibility of integration of the suggested analysis to real-time systems is discussed in Sect. 5.

2 Dynamic Model of the Inverter-Based Microgrid

The microgrid system considered in this work for fault prediction consists of three distributed generation system (DG). Each DG is operated based on the droop-based power sharing that consists of a VSI on common reference frame [9]. The detailed

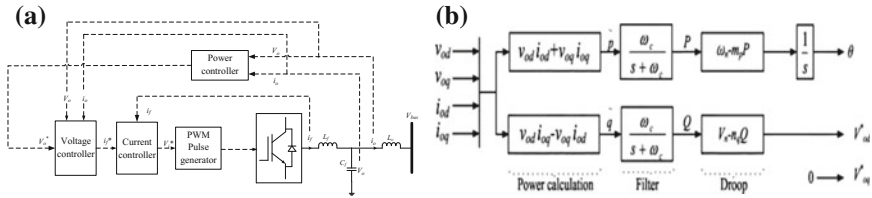


Fig. 1 Block diagram of **a** voltage source inverter model and **b** power controller

model of a single VSI is shown in Fig. 1a which mainly consists of the inverter, output filter, power-sharing controllers, voltage and current controllers. The power-sharing controllers control both the real and imaginary power using droop control of frequency and voltage, respectively, as shown in Fig. 1b. They mainly replicate the governor action as in the case of a synchronous generator. The active power droop control works with the main principle of decreasing active power with the increase in frequency and vice versa [5]. Also, the reactive power droop control works with a similar principle of decreasing reactive power with the increase in the voltage. The conventional controller used is a linear PI controller. The voltage controller along with all its feedback and feed-forward elements with its control action conventionally achieved using PI controllers can be traced from [9].

2.1 Output LC Filter Coupling Inductance Model

The main purpose of the LC filter is that it can remove the high frequency harmonics. Also the LC filter prevents the chance of resonance with the network and load side if chosen according to the system [5]. The coupling inductance mainly reduces the coupling between the active and reactive power components. A single inverter is thus a combination of the DG, power controllers, current and voltage controllers and output LC filter and coupling inductances. The inverter model simulated includes three voltage source inverter of same rating. The three inverters are interconnected through the two transmission lines which are considered as network. The transmission lines are considered to be short transmission lines and are emulated using suitable R-L branch. The inverters are connected to three loads as shown in Fig. 2 with the help of the network. The load considered in this work is resistive load. The inverter parameters are used for the simulation as given in Table 1 and have been adopted from [4, 10].

2.2 Methodology and Simulated Faults

Different fault conditions for the microgrid model are simulated and are shown in Table 2. The output current of the three inverters is recorded in dq reference frame

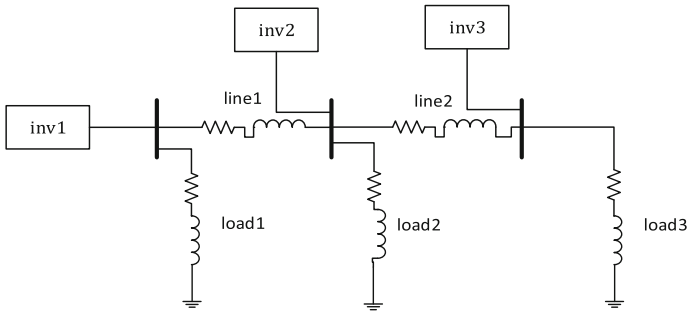


Fig. 2 Complete test system used

Table 1 Inverter parameters used for simulation [10]

Inverter	Parameter	Value
<i>Inverter parameters</i>		
1,2,3	mp, nq	1.57×10^{-6} , 0.002
1,2,3	K_{vi} , K_{vp}	390, 0.05
1,2,3	K_{ci} , K_{cp}	16×10^3 , 10.5
1,2,3	R_n	1000 Ω
<i>Line parameters & load parameters</i>		
Line 1	R_{line1} & X_{line1}	0.23 & 0.1 Ω
Line 2	R_{line2} & X_{line2}	0.35 & 0.58 Ω
Inverter 1	Active power	5.8 kW
Inverter 2	Active power	6.5 kW
Inverter 3	Active power	7.3 kW

Table 2 Different fault conditions simulated

Fault simulated			
Inverter	Type of faults	Fault instant (for training)	Fault instant (for testing)
1,2,3	Line-to-ground (A)	0.3	0.5
1,2,3	Line-to-ground (B)	0.3	0.5
1,2,3	Line-to-ground (C)	0.3	0.5
1,2,3	Line–line–ground (AB)	0.3	0.5
1,2,3	Line–line–ground (BC)	0.3	0.5
1,2,3	Line–line–ground (AC)	0.3	0.5
1,2,3	Line–line–line–ground (ABC)	0.3	0.5
1,2,3	Line–line–line–ground (ABC)	0.3	0.5
1	Line–line–line–ground (ABC)	0.3	0.5
2	Line–line–line–ground (ABC)	0.3	0.5
3	Line–line–line–ground (ABC)	0.3	0.5

and have been used for MF DFA analysis for multifractal feature extraction and fault localization and detection using neural networks. The time series generated by the load currents during normal operation and during different fault conditions and are obtained by the taking the cumulative sum of fluctuations. The time series is analyzed by MF DFA for extracting the multifractal features. The singularity spectrum width of the multifractal spectrum and the Hurst exponent quantifying the long-run correlations are the extracted features of the time series which is tested with analysis of variance (ANOVA) validating the efficacy of the features' and fed to artificial neural network (ANN) model for fault detection.

3 Theory

3.1 Multifractal Detrended Fluctuation Analysis (MF DFA)

The time series generated by the load events are analyzed using MF DFA. The steps involved in MF DFA are summarized as follows. Let us consider $y(n)$ to be a non-stationary, nonlinear time series of length N [11]. The mean value of the time series is given by Eq. (2).

$$\bar{y} = \frac{1}{N} \sum_{n=1}^N y(n) \tag{1}$$

The integrated time series is computed by subtracting the mean value from the signal as shown in Eq. (2).

$$X(i) = \sum_{n=1}^i [y(n) - \bar{y}] \forall i \in 1, 2, \dots, N \tag{2}$$

The next step consists in dividing the time series into N_s non-overlapping segments, where s denotes the segment length and $N_s = \text{int}(N/s)$. For N not divisible by s , a section of data sequence is left out. For including the left out data, the procedure is reiterated from the reverse end and thus rendering $2N_s$ number of segments. Using least square polynomial approximation, the variation in local trends for each of the $2N_s$ is computed for each sequence fragments as shown in Eq. (3).

$$F^2(s, v) = \frac{1}{s} \sum_{i=1}^s \{X[(v-1)s + i] - x_v(i)\}^2 \text{ where } v = 1, 2, \dots, N_s \tag{3}$$

where $x_v(i)$ signifies the least square fitted value in the v th segment. By taking the average of $2N_s$ segments the q th order fluctuation function, $Fq(s)$ is computed, where q is the scaling index as given by Eq. (4).

$$F_q(s) = \left\{ \frac{1}{2Ns} \sum_{\nu=1}^{2Ns} [F^2(s, \nu)]^{0.5q} \right\}^{1/q} \quad (4)$$

Since, $F_q(s)$ depends on both the values of q and time scale s , its variation is analyzed using a log–log plot. It is computed for all time-scale range [10]. When the $y(n)$ is long-range power-law correlated, then $F_q(s)$ versus s shows a power-law variation with a slope as function of $H(q)$ as shown in Eq. (6). For $H(q)$ being the generalized Hurst exponent

$$F_q(s) \propto s^{H(q)} \quad (5)$$

For monofractal time series, the scaling behavior of $F_2(s, \nu)$ is similar for all segments and for all values of q which means that $H(q)$ is independent of q . But, for a multifractal time series, $H(q)$ is a function of q and the Hurst exponent is taken for $q = 2$, and the scaling characteristics of segmental fluctuation is described by $H(q)$ for all values of q .

3.2 Multifractal Spectrum

The long-range correlations of a monofractal time series are characterized by a single Hurst exponent with the multifractal scaling exponent $\tau(q)$ showing linear dependency on the scaling exponent q . The multifractal scaling exponent $\tau(q)$ is related with the generalized Hurst exponent $H(q)$ by the relation shown in Eq. (6).

$$\tau(q) = qH(q) - 1 \quad (6)$$

While a multifractal time series is a set comprising of multiple Hurst exponents and there is nonlinear dependency of $\tau(q)$ on q as reported in [11]. With the help of Legendre transform, the relationship between singularity spectrum $f(\alpha)$ and scaling exponent $\tau(q)$ is obtained as given in Eq. (8).

$$\alpha = d\tau/dq \ \& \ f(\alpha) = q\alpha - \tau(q) \quad (7)$$

where α is the singularity exponent and $f(\alpha)$ signifies the fractal dimension of series subset characterized by α . Mathematically, α and $f(\alpha)$ can be expressed in terms of $H(q)$ as given by Eq. (8)

$$\begin{aligned} \alpha &= H(q) + q(q) \\ f(\alpha) &= q[\alpha - H(q)] + 1 \end{aligned} \quad (8)$$

The singularity spectrum $f(\alpha)$ of the multifractal spectrum determines the long-range correlation property of a time series. The width of the multifractal

spectrum quantifies the multifractality of the spectrum. A large spectral width is associated with a high degree of multifractality and vice versa. Since $H(q)$ is independent of q for a monofractal time series; hence, the multifractal spectrum width will be zero [12].

3.3 Artificial Neural Network (ANN)

ANN inspired from biological computations consists of a multilayered weighted combination of signals coming from a cluster of neural units called neurons. The self-learning tuning of the weights of the network paths with different activation functions coupled with a threshold function limit false triggers before propagating to other neurons provides an excellent nonlinear feature learning methodology where traditional learning fails. Mathematically, it is expressed as Eq. (10).

$$y_i = \sum_{m=1}^{L_i} \left[\omega_{ij} \sigma \left(\sum_{k=1}^n h_{jk} i_{ok} + \varphi_{vj} \right) + \theta_{wi} \right] \text{ where } i = 1, 2, \dots, n \quad (10)$$

where i_{ok} and y_i are the output currents and output of the ANN and h_{jk} and w_{ij} are hidden and output layer weights. The weights of these interconnections are updated in the learning process. Details about the application of ANN to microgrid fault prediction can be found in [8, 13, 14].

4 Observations

4.1 Line Faults in Inverters

Line faults in an inverter are marked by increase in output current to the saturation level. Faults occurring for a very short duration are difficult to detect with an ANN. Number of inputs and outputs of the ANN is 6 which is same as that of the number of output currents (I_{od1} , I_{oq1} , I_{od2} , I_{oq2} , I_{od3} , I_{oq3}) while the optimum number of hidden layers is determined by prior iterations and maximizing the accuracy. More details can be found in [8].

4.2 MF DFA Features

During normal operation of a microgrid, all the load currents exhibit anti-persistent ($H(q=2) < 0.5$) and similar generalized Hurst exponent scaling behavior and multifractal spectrum characteristics. But when fault occurs in any inverter, the load

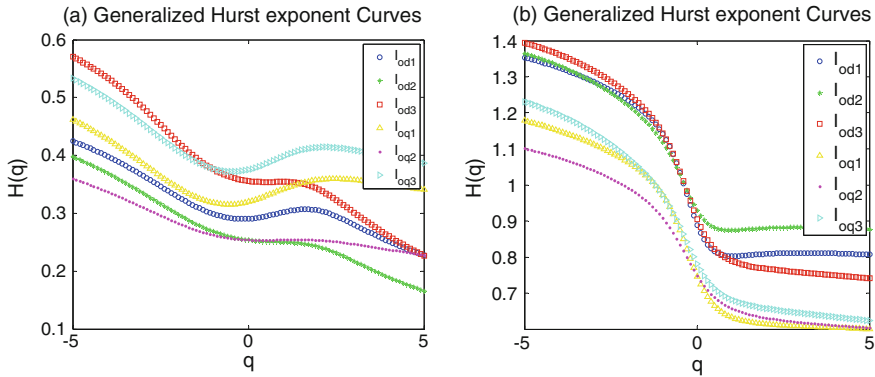


Fig. 3 Generalized Hurst exponent curves of the Iod’s a normal operation b line fault at DG3

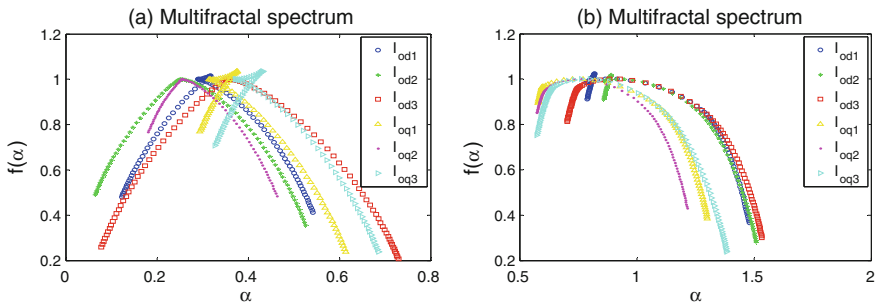


Fig. 4 Multifractal spectrum of the Iod’s a normal operation b line fault at DG3

lines supplying current to the fault areas gets interrupted and as such their fractal nature changes. These changes are manifested in the Hurst exponent and spectrum width values. Analyzing these changes in multifractal features of the load currents and fault localization is done in the microgrid by a neural network model. The generalized Hurst exponent curves and the multifractal spectrum of the normal and fault load currents are shown in Figs. 3 and 4, respectively.

5 Conclusions

The inherent fractal nature of the time series generated during normal operation and fault events of a microgrid has been characterized by MFDFA analysis. The Hurst exponent and the multifractal spectrum parameters are trained with ANN for fault detection in microgrids. Also, the extreme behavior of windowed fractal analysis

for finding the exact instant of fault localization is being studied for autonomous operation and integration to real systems.

References

1. Jayawarna, Nilanga, et al. "Safety analysis of a microgrid", 2005 International Conference on Future Power Systems, IEEE (2005).
2. Bo, Z. Q., et al. "Transient based protection for power transmission systems", Power Engineering Society Winter Meeting, 2000, Vol. 3 (2000).
3. Maria, Tim C. Green, and John DF McDonald, "Modeling and analysis of fault behavior of inverter microgrids to aid future fault detection", IEEE International Conference on System of Systems Engineering (2007).
4. Nagaraju Pogaku, Milan Prodanovic and Timothy C. Green, "Modeling, Analysis and Testing of Autonomous Operation of an Inverter-Based Microgrid", IEEE Transactions on Power Electronics, Vol. 22, No. 2, March (2007).
5. SalomonssonDaniel, LennartSoder, and AmbraSannino, "Protection of low-voltage DC microgrids", IEEE Transactions on Power Delivery, Vol. 24, no. 3, pp. 1045–1053 (2009).
6. DewadasaManjula, Arindam Ghosh, and Gerard Ledwich, "Line protection in inverter supplied networks", Power Engineering Conference, AUPEC'08, Australasian Universities (2008).
7. J. Chen, and J. Hou. "SVM and PCA based fault classification approaches for complicated industrial process", Neurocomputing 167, pp. 636–642 (2015).
8. A. Shankar, "Toward intelligent fault classification in autonomous microgrids", Industry Applications Society Annual Meeting, IEEE (2015).
9. D. Pullaguram, M. Mukherjee, S. Mishra, N. Senroy, "Non-linear fractional order controllers for autonomous microgrid system", IEEE 6th International Conference on Power Systems (ICPS), India, March (2016).
10. M. Mukherjee, D. Pullaguram, S. Mishra, "Dynamic droop based inverter control for autonomous microgrid", Biennial International Conference on Power and Energy Systems: Towards Sustainable Energy (PESTSE), India, January (2016).
11. Kantelhardt, Jan W., et al. "Multifractal detrended fluctuation analysis of nonstationary time series", Physica A: Statistical Mechanics and its Applications, Vol. 316, no. 1, pp. 87–114 (2002).
12. E. A. F. Ihlen. "Introduction to multifractal detrended fluctuation analysis in Matlab", Fractal Analyses: Statistical and Methodological Innovations and Best Practices, pp. 97 (2012).
13. Hopfield, John J., "Artificial neural networks", IEEE Circuits and Devices Magazine, Vol. 4, no. 5, pp. 3–10 (1988).
14. Mitchell, Tom M. "Artificial neural networks", Machine learning 45, pp. 81–127 (1997).